



TITLE:

QUANTITATIVE STUDY OF THE DISSIPATIVE TODA LATTICE : Preliminary results(Toda Lattice and the Related Topics)

AUTHOR(S):

Kuusela, T.; Hietarinta, J.

CITATION:

Kuusela, T. ...[et al]. QUANTITATIVE STUDY OF THE DISSIPATIVE TODA LATTICE : Preliminary results(Toda Lattice and the Related Topics). 数理解析研究所講究録 1988, 650: 29-45

ISSUE DATE:

1988-04

URL:

<http://hdl.handle.net/2433/100330>

RIGHT:

QUANTITATIVE STUDY OF THE DISSIPATIVE TODA LATTICE

- preliminary results -

T. Kuusela and J. Hietarinta⁺

Wihuri Physical Laboratory
and
Department of Physical Sciences
University of Turku
Turku
FINLAND

Abstract: We discuss the effects that a finite dissipation has on the behavior of a soliton in the Toda-lattice. From both numerical and experimental results we find e.g. a noticeable tail effect, which has not yet been explained theoretically.

1. Introduction

We are now celebrating the 20th anniversary of the Toda lattice model [1]. It has turned out to be a fruitful prototype of a discrete integrable model, and has been studied intensively. It has also been generalized into various directions (see e.g. the integrable Toda molecules, Sec. 3.3.2, 3.4.4 and 3.5.2 in [2] and references therein).

The continuum limit of the Toda lattice model is given by the Korteweg - de Vries [3] or Boussinesq [4] models. Thus one can study also some effects of the continuum models using discrete methods, and vice versa.

An attractive feature of the Toda lattice is that it has a simple experimental realization through an LC-lattice, as was first proposed by Hirota and Suzuki [5]. This provides us with perhaps the easiest experimental method to see various soliton phenomena [6].

⁺ Supported by the Academy of Finland and Ministry of Trade and Industry

2. Experimental realization

The experimental system consists of a chain of LC-circuits (Fig. 1) in which the voltage dependency of C is nonlinear. The nonlinearity is described by [7]

$$C(V) = Q(V_0)/(F(V_0)-V_0+V). \quad (1)$$

The circuit equations are:

$$L\partial_t I_n = V_{n-1} - V_n, \quad \partial_t Q_n = I_n - I_{n+1}, \quad (2)$$

$$Q_n = \int_{V_0}^{V_0+V_n} C(v) dv,$$

which together with (1) imply

$$LQ(V_0)\partial_t^2 \ln[1+V_n/F(V_0)] = V_{n-1} + V_{n+1} - 2V_n. \quad (3)$$

This can be further transformed by

$$V_n = v_n F_0, \quad t = [LQ_0/F_0]^{1/2} \tau \quad (4)$$

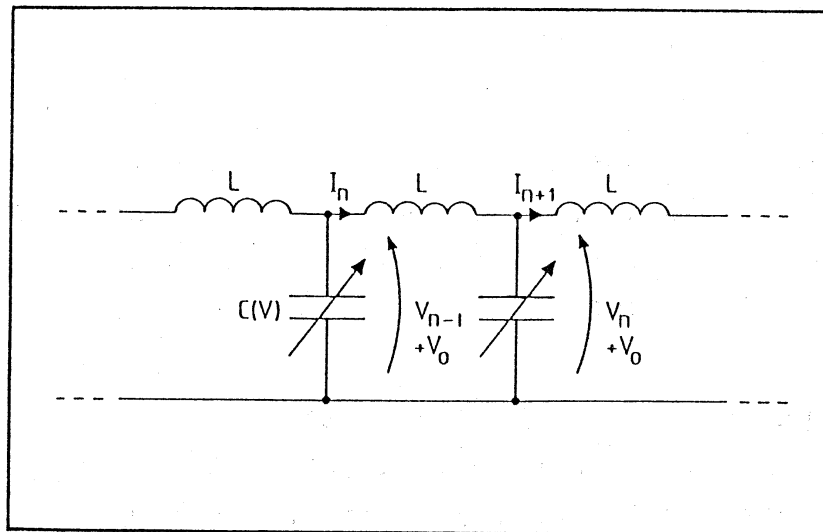


Fig. 1. Part of the nonlinear transmission line.

$[Q_0 = Q(V_0), F_0 = F(V_0)]$ to the canonical dimensionless form

$$\partial_\tau^2 \ln(1+v_n) = v_{n-1} + v_{n+1} - 2v_n, \quad (5)$$

from which the original Toda lattice is obtained by the substitution $\log(1+v_n) = x_n - x_{n+1}$. With this circuit it is easy to observe such basic soliton phenomena as initial pulse decomposition into solitons and soliton scattering [6].

3. Dissipation

In a real system there are always some losses, nonuniformities and other effects that cause deviations from the ideal system. In practice it seems that the resistance in L causes most trouble. Such dissipative effects have been studied for the Korteweg - de Vries equation [8] and for the Toda lattice [9,10,11].

The circuit diagram in the case of a nonzero resistance and conductance is given in Fig. 2; the equations in this case are:

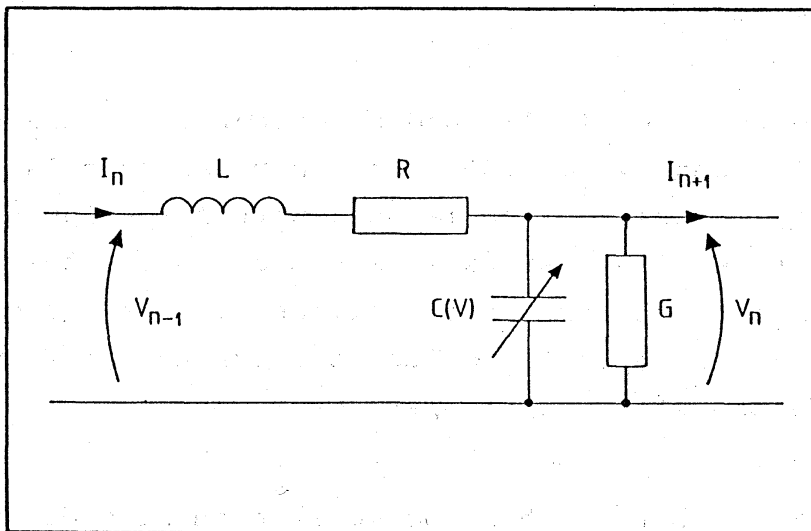


Fig. 2. Part of the transmission line with resistance R and conductance G .

$$\begin{aligned} L\partial_t I_n + R I_n &= V_{n-1} - V_n, \\ \partial_t Q_n + G V_n &= I_n - I_{n+1}, \end{aligned} \quad (6)$$

which can be transformed by (4) to

$$\partial_t^2 \ln(1+v_n) + \tilde{R} \partial_t \ln(1+v_n) + \tilde{G} \partial_t v_n + \tilde{R}\tilde{G} v_n = v_{n-1} + v_{n+1} - 2v_n \quad (7)$$

where $\tilde{R} = R/R_0$, $\tilde{G} = GR_0$, and $R_0 = (LF_0/Q_0)^{1/2}$.

A formal continuum limit of (7) yields [3]

$$u_{xxx} - 6uu_x + u_{t^*} + (12/t^*)u = 0, \quad (8)$$

where

$$(t^*)^{-1} = (R/L + G/C_0)/v_0 \quad (9)$$

$$v_0 = (LC_0)^{-1/2} \quad (10)$$

Later we will discuss how good an approximation this continuum limit really is.

4. Numerical results

We have studied numerically and experimentally the behavior of solitons described by Eq. (6). For numerical calculations we used the four step Adams-Moulton method with Adams-Bashfort corrections. The first four steps were obtained by the Runge-Kutta method. It should be noted that soliton equations are usually not well behaved in numerical studies, because as stiff systems they tend to have bad stability properties.

Figs. 3 to 6 illustrate how the soliton changes due to dissipation. We have given the soliton at various lattice points for $R = 5, 10, 20$ and 50 Ohms. The amplitude is given in Volts as a function of time in nanoseconds. An ideal soliton was put in the lattice centered at lattice point 12 at $t=0$. The initial

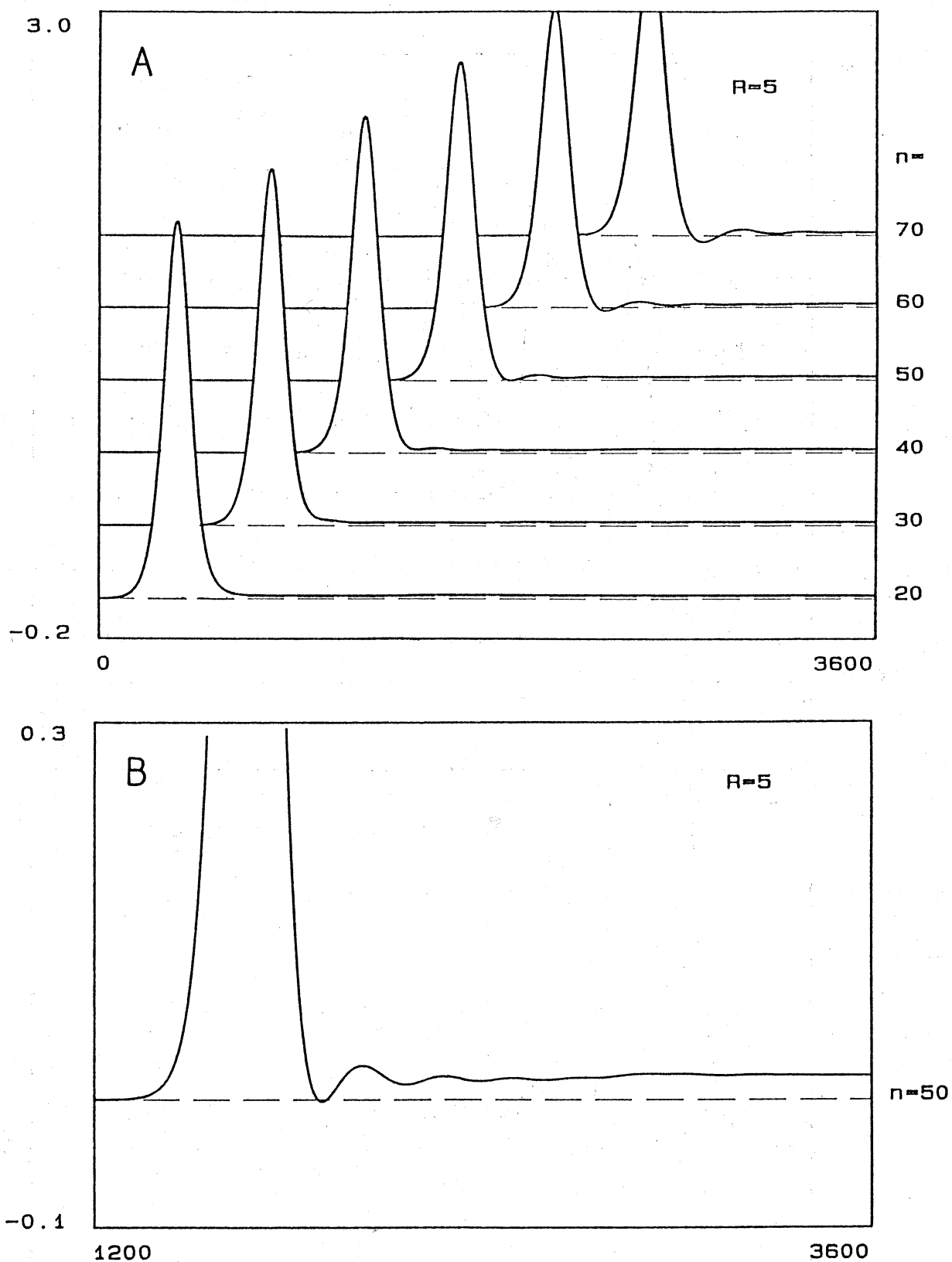


Fig. 3. A: Results from numerical integration of (6) at various lattice points for $R = 5$ Ohms, $L = 22 \mu\text{H}$, $Q_0 = 583 \text{ pC}$, $F_0 = 6.2 \text{ V}$. The initial soliton with an amplitude of 2 Volts was centered at lattice point 12 at $t = 0$. B: An enlargement at lattice point 50.

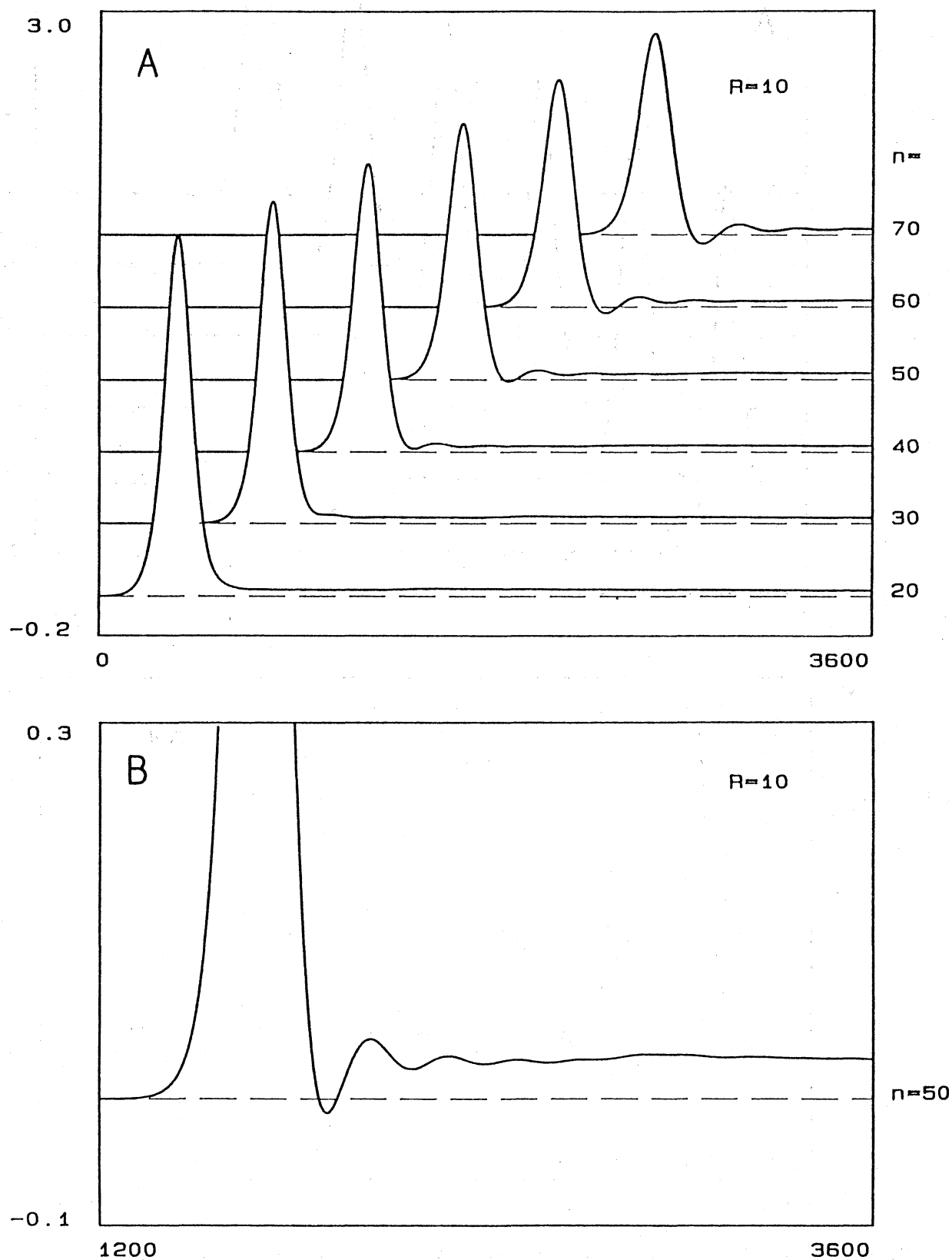


Fig. 4. Same as Fig. 3 but $R = 10$ Ohms.

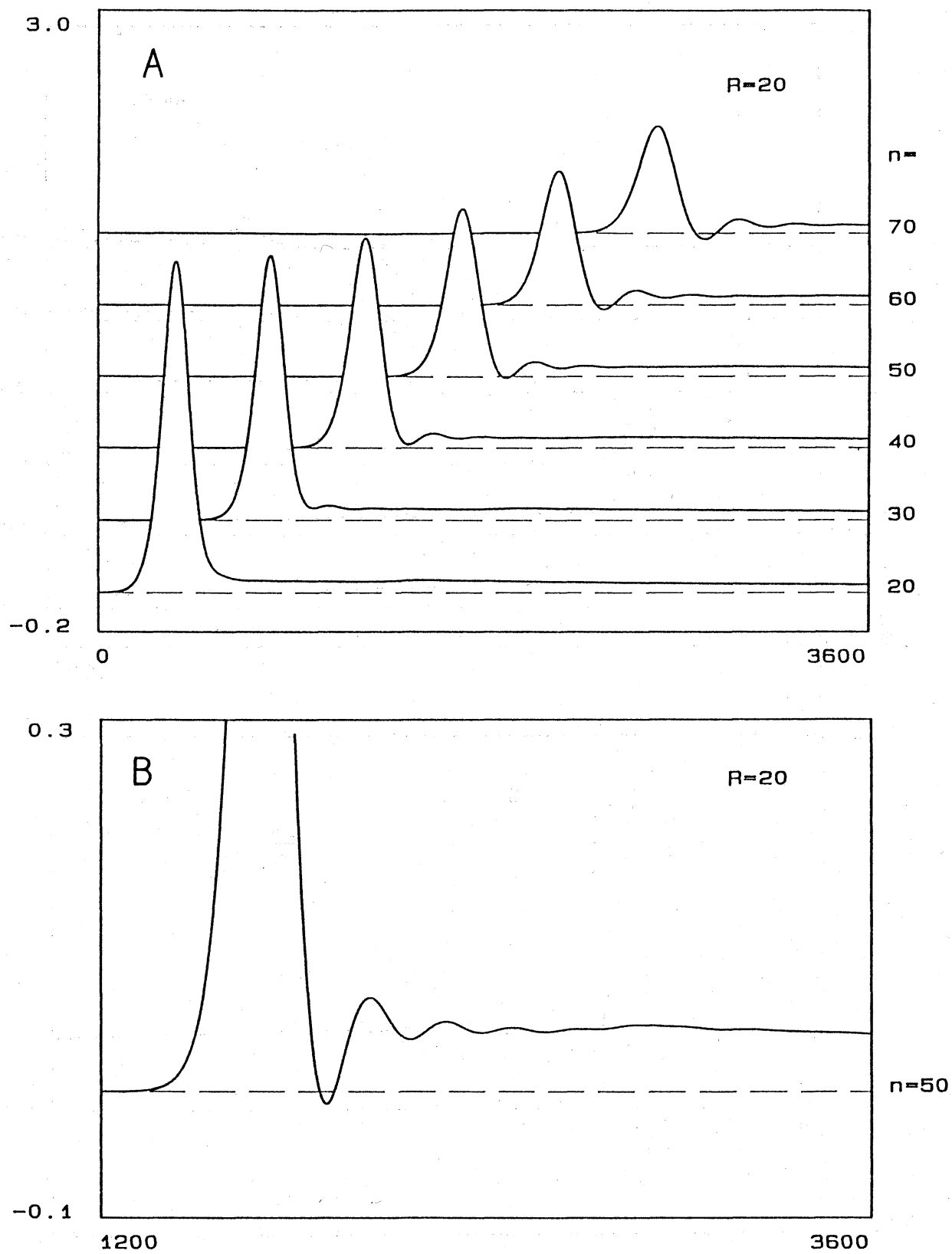


Fig. 5. Same as Fig. 3 but $R = 20$ Ohms.

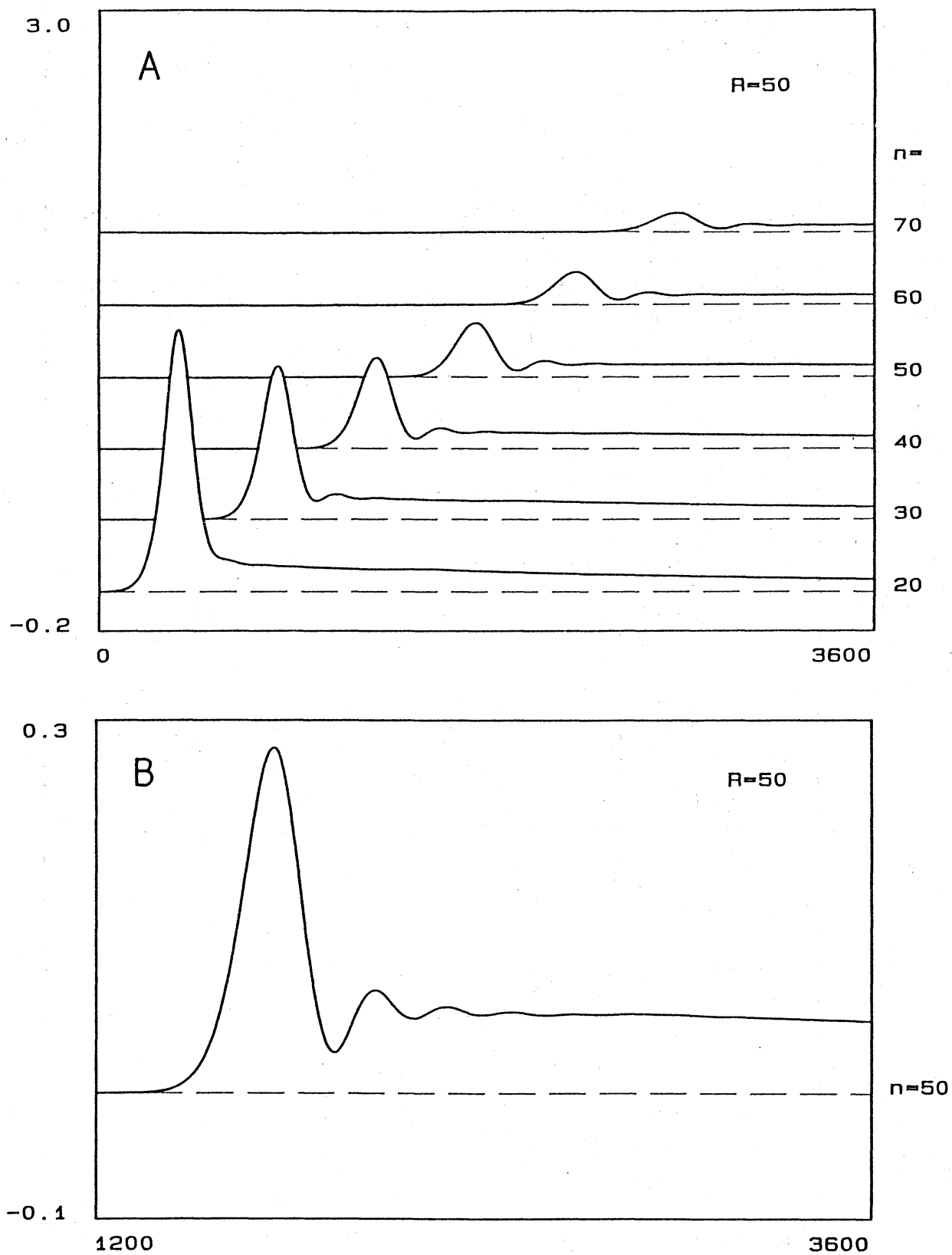


Fig. 6. Same as Fig. 3 but $R = 50$ Ohms.

amplitude was in each case 2 Volts. An enlargement of the situation at lattice point 50 is also displayed.

The main new feature is the raised tail which decreases slowly. The oscillations around this tail increase initially as a function of lattice point, but decrease quickly at each lattice point. The oscillations depend strongly on the type of the initial pulse: For Fig. 7 we have fed a square pulse in the lattice and as a consequence the oscillations are much stronger, but the average tail is as before.

The effects caused by nonzero conductance are quite different. In Fig. 8 we have results from numerical integration of (6) with $R=0$, $G = 9.3 \cdot 10^{-5} \text{ Ohms}^{-1}$. Note that the tail has opposite sign.

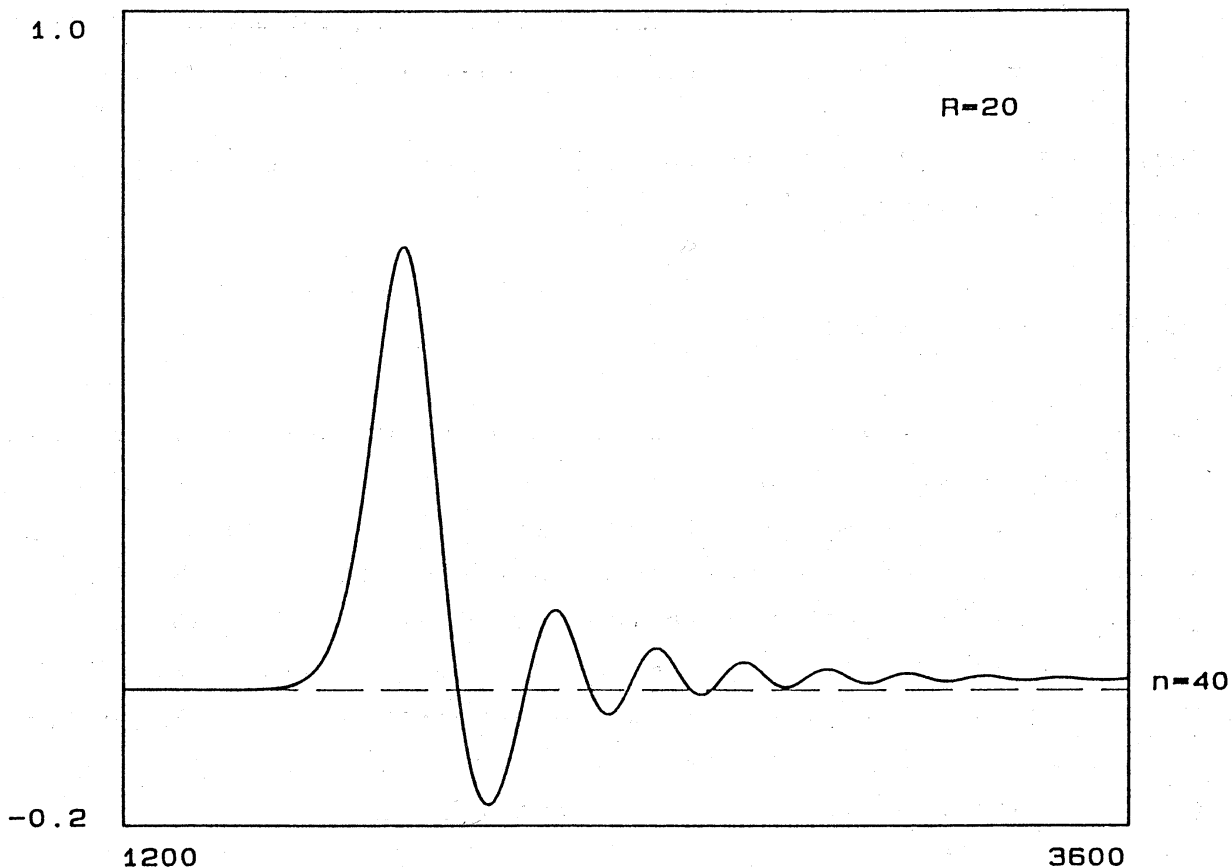


Fig. 7. The solution of (6) when a square pulse (width 135 ns, amplitude 2 Volts) was fed to the beginning of the transmission line. $R = 20 \text{ Ohms}$.

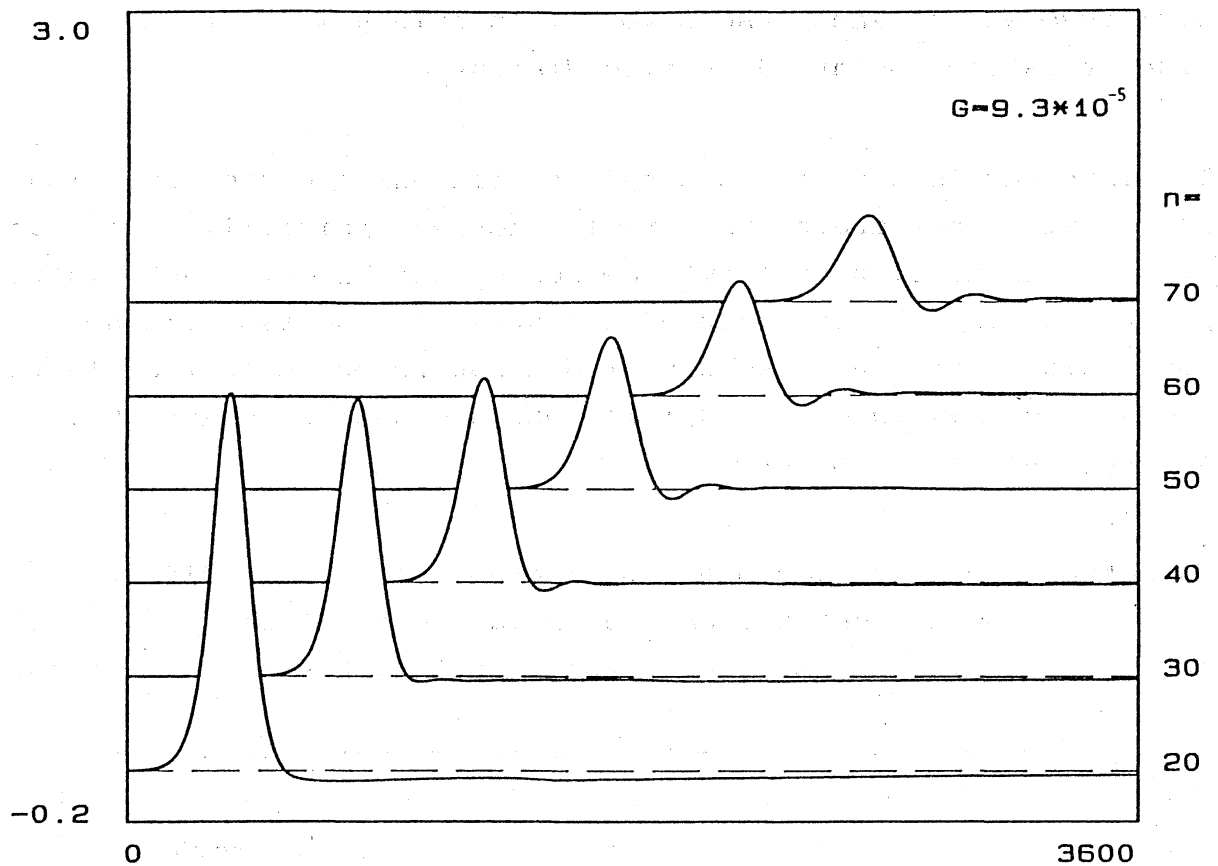


Fig. 8. The solution of (6) for $R = 0$, $G = 9.3 \times 10^{-5} \text{ Ohms}^{-1}$, otherwise as in Fig. 3.

5. Experimental results

To find out how well a real system is described by equations (6,7) we constructed an experimental LC lattice with commercially available components. For $C(V)$ in (1) we found at $V_0 = 1.5 \text{ V}$ the following characteristic constants: $F_0 = 6.2 \text{ V}$, $Q_0 = 583 \text{ pC}$, $C_0 = 94 \text{ pF}$. These values imply $v_0 = 2.2 \cdot 10^7 \text{ 1/s}$ and $R_0 = 484 \text{ Ohms}$. The series resistance R was variable between 5 and 55 Ohms and $L = 22 \text{ } \mu\text{H}$. The experimental measurements were made through a gated integrator and boxcar averager. This improved the data considerably from what has been observed so far.

Experimental results with $R = 10$ and 20 Ohms are given in Figs. 9 and 10 at various lattice points and with enlargements at lattice point 50. A square pulse ($V_{in} = 4 \text{ V}$, $dt = 140 \text{ ns}$) was fed at the beginning of the lattice, by lattice point 20 it had already

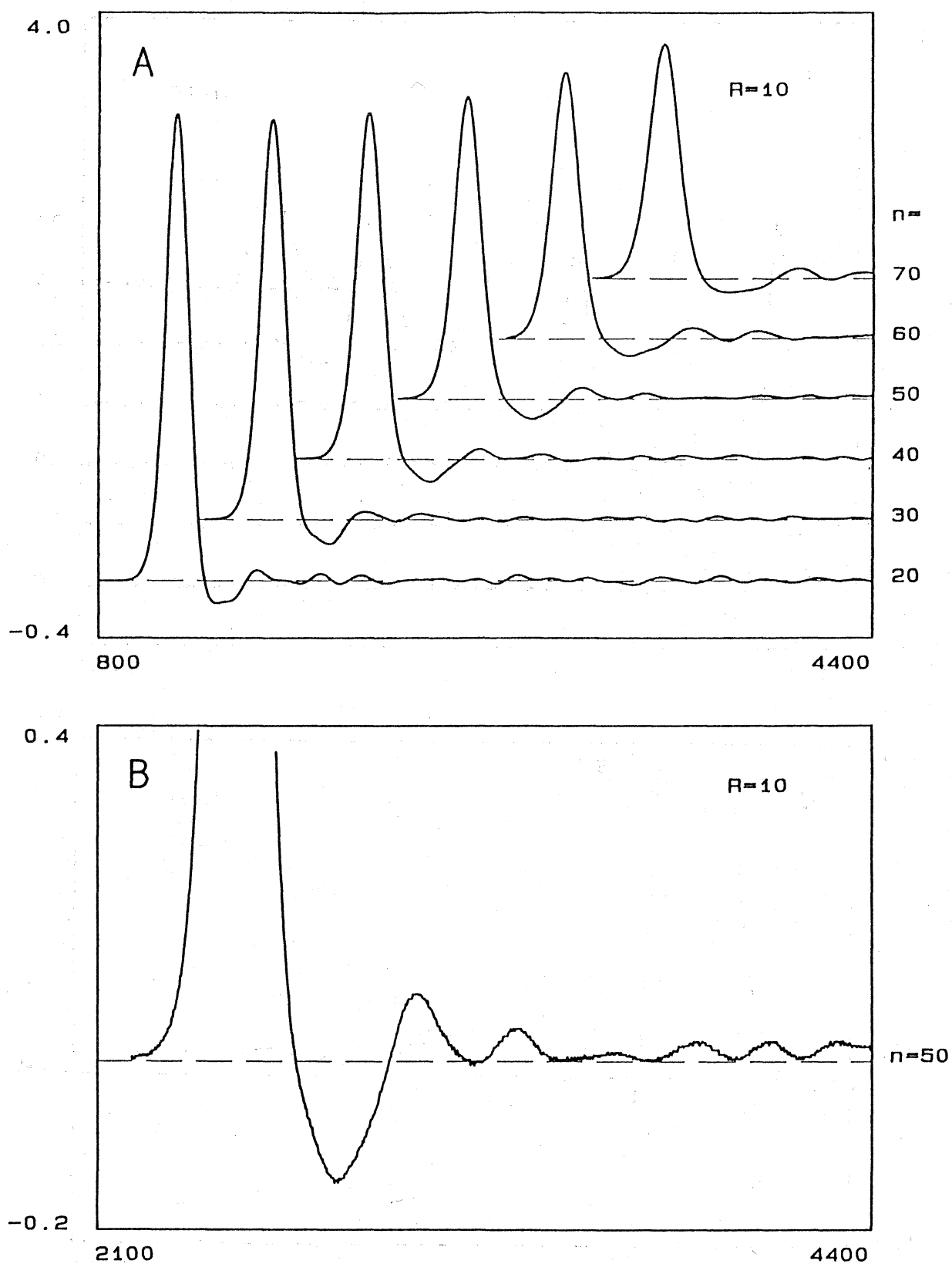


Fig. 9. A: Experimental measurements at various lattice points for $R = 10$ Ohms. A square pulse (width 140 ns, amplitude 4 Volts) was fed to the beginning of the line. B: Enlargement of the situation at lattice point 50.

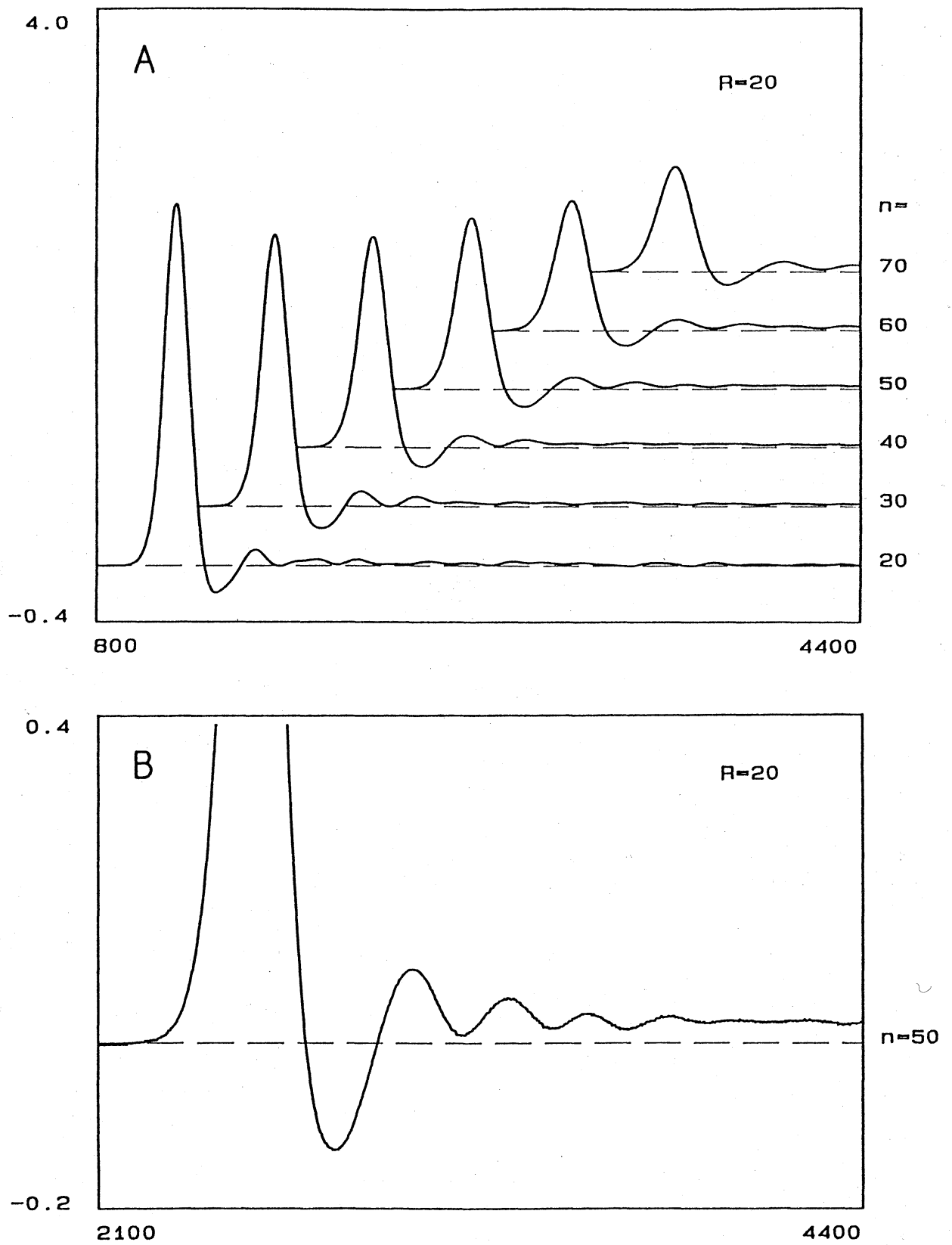


Fig. 10. Same as Fig. 9 but $R = 20$ Ohms.

obtained the shape of a soliton. The noise is very small as can be seen in the enlarged figures. The jaggedness in the curve is about .1% of the size of the soliton, while in the oscilloscope screen the noise is typically 4%.

6. Characterization of the data

The observed pulse can be divided into a soliton part and a tail part. The soliton part is (at least initially) close to the ideal soliton. To characterize it one should be able to describe the time dependence of its amplitude, half width, and speed. In a system without dissipation these properties have definite relationships, but in a real system some deviations are expected.

At each lattice point the soliton part is followed by a tail part. The tail is best described by a slowly decaying basic level together with exponentially decaying oscillations around it. We have found that at each lattice point the tail can be well described with the function

$$V_{\text{tail}}(t) = B \exp(-bt) + C \exp(-ct) \cos[(d + f \exp(-gt))t] \quad (11)$$

As functions of the lattice point b , d and g are almost constant, f and B are slowly varying functions, but C and c do not seem to have simple behavior. C and c depend also strongly on the initial pulse shape, compare Figs. 5 and 7.

7. Problems in the theoretical description

In the continuum limit of the Toda lattice both parallel and series resistance contribute the same way (8,9), but numerical results from (6) show that they have different effects, in particular for the tail (compare Figs. 3 and 8). Thus the continuum limit destroys some essential features of the dissipative Toda lattice, and one cannot expect any method starting from (8), like the Karpman-Maslov (KM) method [12], to explain the tail, not even in the limit when R and G are small.

Even though the KM method fails for the tail, it might be able to describe the slow decay of the soliton part. To test this we have in Fig. 11 compared the KM-solution and the numerical results (with the same initial conditions). The ideal soliton is included as a reference. The velocity and amplitude of the soliton, as calculated from KM-theory, are near the numerical solution, but obviously there is room for improvement.

Kako has treated the dissipative Toda lattice using perturbation theory for the inverse scattering transform [9]. Due to its starting point this method should be able to differentiate between resistance R and conductance G . Unfortunately Kako's solution for the soliton tail is very complicated, and in any case

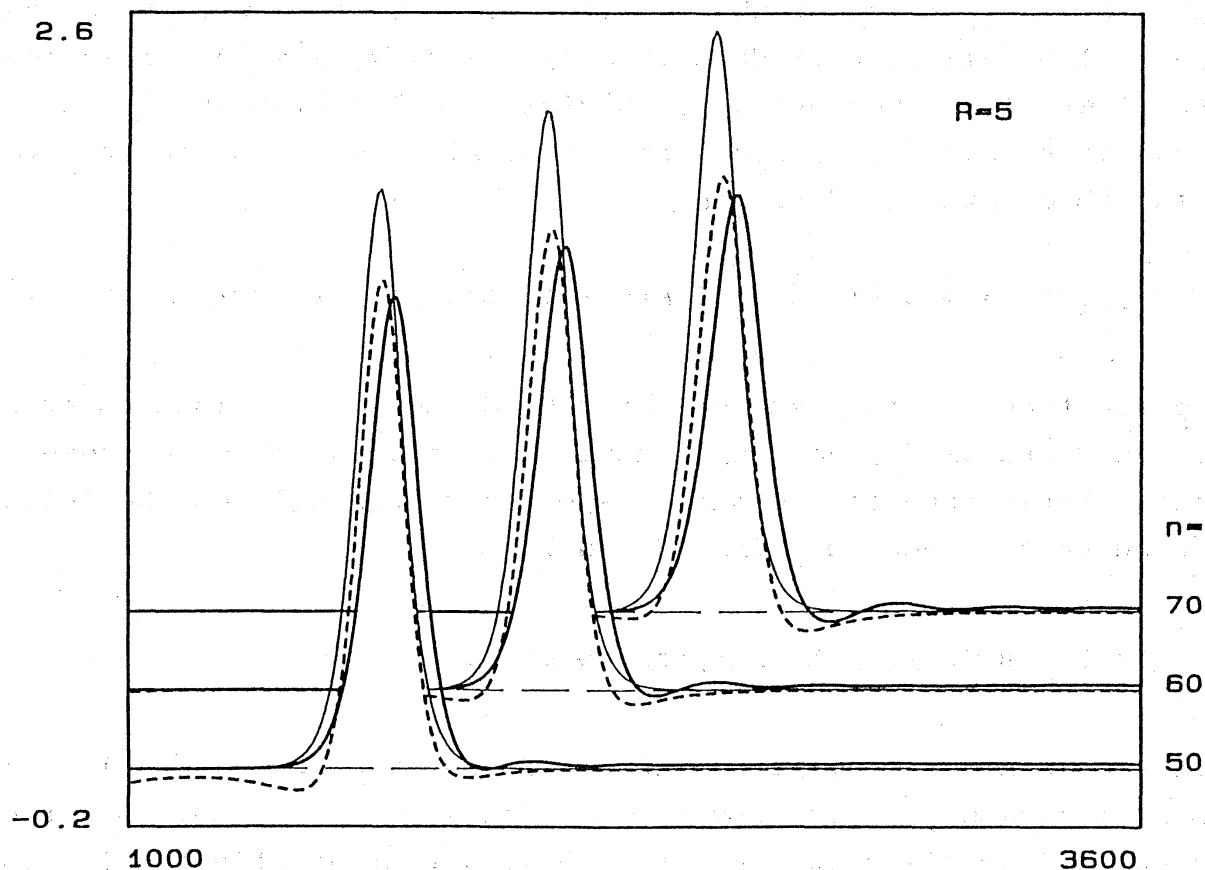


Fig. 11. The Karpman-Maslov solution (dashed line), numerical results (solid line) and the ideal soliton without dissipation (thin line) with the same initial conditions as in Fig. 3.

the sign of the tail is negative everywhere (see Fig. 3 in Ref. [9]) regardless of the values of R and G . [There is another troublesome feature in the case of $G = 0$ and nonvanishing R : the time development of the additional eigenvalue is not as expected (see Fig. 2 in Ref. [9])].

Kako's predictions for the main soliton part are given in Fig. 12. The results are somewhat more accurate than those obtained from the KM-theory.

Since the soliton part is fairly accurately described by both KM and Kako we have analyzed it further by calculating the logarithmic derivative of the soliton amplitude, $k = (L/R) d_t A/A$. The results are shown in Figs. 13 and 14 with $R = 2$ and 5 Ohms. The k quantity seems to have two limit values. In the case of small

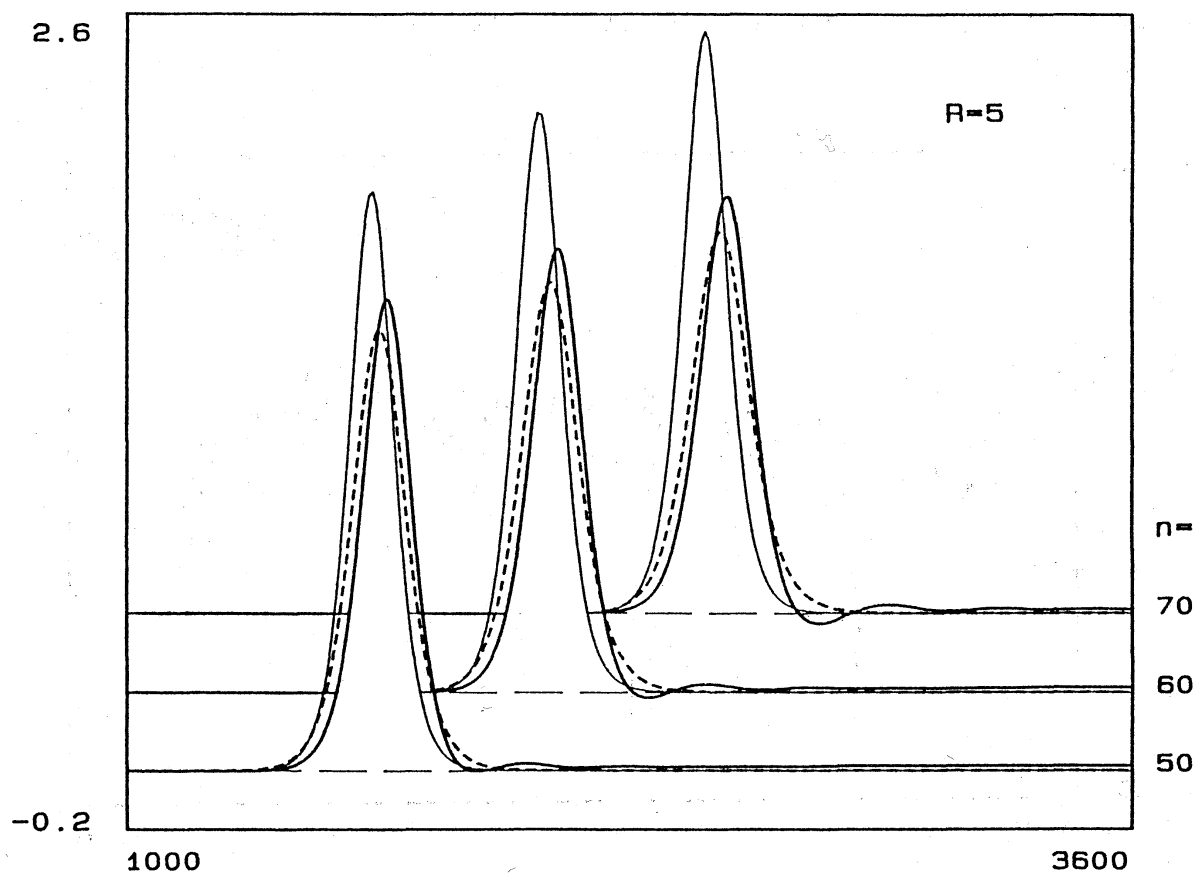


Fig. 12. The soliton part of the solution calculated by Kako's theory (dashed line), otherwise as Fig 11.

dissipation and large amplitude k approaches the KM and Kako value $2/3$ for the soliton part. In the limit of strong dissipation and small amplitude k has value $1/2$, which can be obtained from the damping of a linear wave. Note also that the curves for the same resistance but different initial amplitudes seem to have a common envelope curve. This curve is reached rather quickly and its very existence suggests that there is a solution which does not depend on the details of the initial condition.

8. Conclusions

In this article we have described our preliminary results on the behavior of solitons in the dissipative Toda lattice. Apart from the expected decay in the amplitude of the soliton one observes that the soliton has a slowly decaying positive tail. The perturbative methods of Karpman - Maslov and Kako give a qualitative explanation for the decay of the soliton, but fail on the finer details, e.g. in the description of the tail.

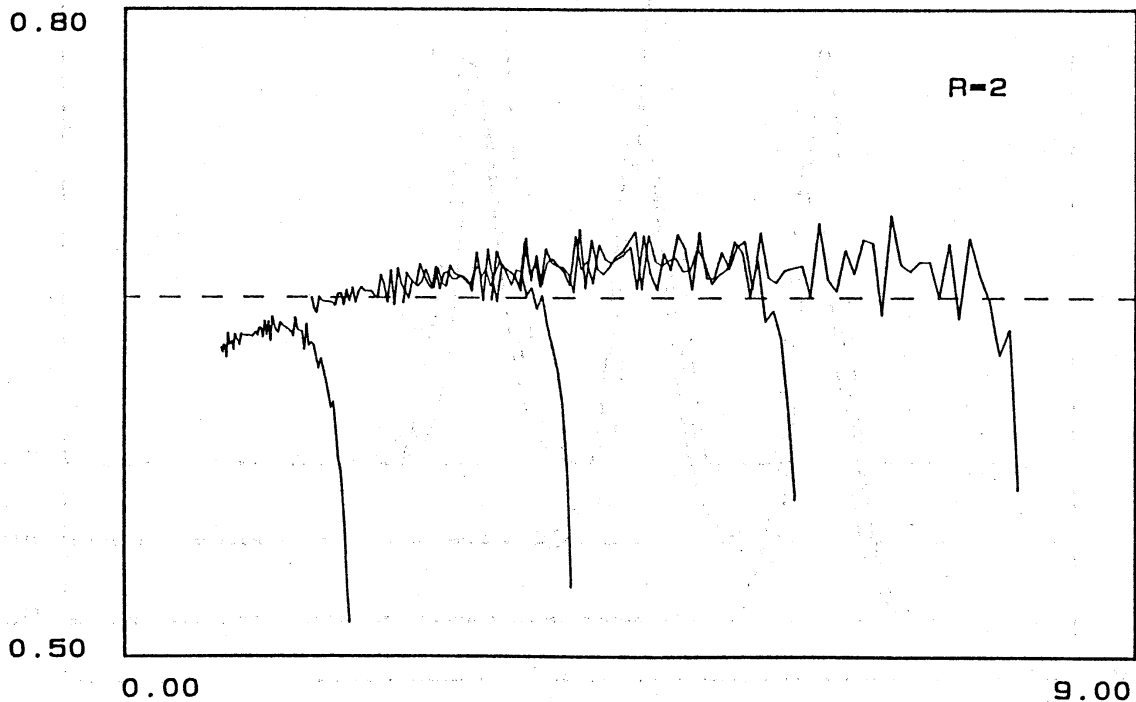


Fig. 13. The logarithmic derivative of the soliton amplitude as a function of the amplitude from numerical integration, $R = 2$ Ohms.

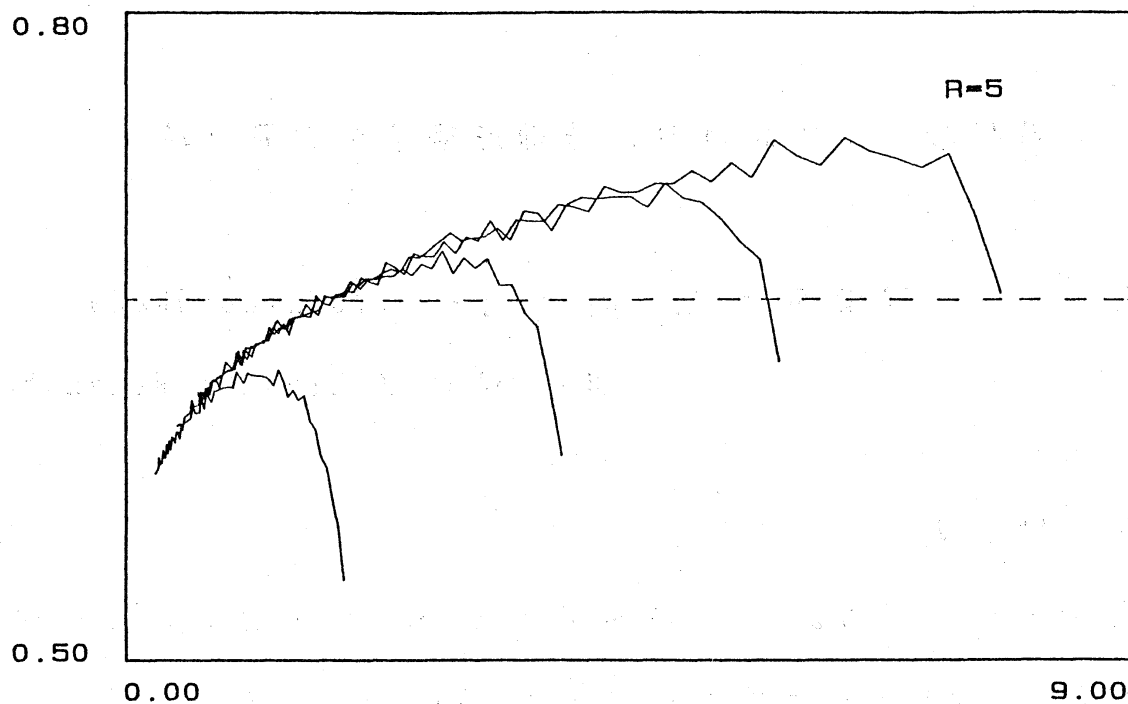


Fig. 14. Same as Fig. 13 but $R=5$ Ohms.

REFERENCES

- [1] M. Toda, J. Phys. Jpn 22, 431 (1967).
- [2] J. Hietarinta, Phys. Rep. 147, 87 (1987).
- [3] M. Toda, M. Wadati, J. Phys. Jpn 34, 18 (1973).
- [4] T. Taniuti, C-C. Wei, J. Phys. Jpn 24, 941 (1968).
- [5] R. Hirota, K. Suzuki, J. Phys. Jpn 28, 1366 (1970); *ibid* PIEEE 61, 1483 (1973).
- [6] T. Kuusela, J. Hietarinta, K. Kokko, R. Laiho, Eur. J. Phys. 8, 27 (1987).
- [7] H. Nagashima, Y. Amagishi, J. Phys. Jpn 45, 680 (1978).
- [8] S. Watanabe, J. Phys. Jpn 45, 2761 (1978).
- [9] F. Kako, J. Phys. Jpn 47, 1686 (1979).
- [10] H. Nagashima, Y. Amagishi, J. Phys. Jpn 47, 2021 (1979).
- [11] N. Saitoh, Y. Watanabe, J. Phys. Jpn 50, 1774 (1980).
- [12] V. Karpman, E. Maslov, Sov. Phys. JETP 46, 281 (1977); *ibid* 48, 252 (1978).